

1 Proactive selective attention across competition contexts

2 **Authors:** Blanca Aguado-López ^a, Ana F. Palenciano ^a, José M.G. Peñalver ^a, Paloma Díaz-
3 Gutiérrez ^b, David López-García ^c, Chiara Avancini ^a, Luis F. Ciria ^a, María Ruz ^{a,*}

4 ^a *Mind, Brain and Behavior Research Center (CIMCYC), University of Granada, Granada
5 18071, Spain*

6 ^b *Department of Management, Faculty of Business and Economics, University of Antwerp, 2000,
7 Belgium*

8 ^c *Data Science & Computational Intelligence Institute, University of Granada, CP 18071, Spain*

9 *** Corresponding author:** María Ruz (mruz@ugr.es)

10 **Abstract**

11 Selective attention is a cognitive function that helps filter out unwanted information. Theories
12 such as the biased competition model (Desimone & Duncan, 1995) explain how attentional
13 templates bias processing towards targets in contexts where multiple stimuli compete for
14 resources. However, it is unclear how the anticipation of different levels of competition
15 influences the nature of attentional templates, in a proactive fashion. In this study, we used EEG
16 to investigate how the anticipated demands of attentional selection (either high or low stimuli
17 competition contexts) modulate target-specific preparatory brain activity and its relationship
18 with task performance. To do so, participants performed a sex judgement task in a cue-target
19 paradigm where, depending on the block, target and distractor stimuli appeared simultaneously
20 (high competition) or sequentially (low competition). Multivariate Pattern Analysis (MVPA)
21 showed that, in both competition contexts, there was a preactivation of the target category to
22 select with a ramping-up profile at the end of the preparatory interval. However, cross-
23 classification showed no generalization across competition conditions, suggesting different
24 preparatory formats. Notably, time-frequency analyses showed differences between anticipated
25 competition demands, reflecting higher theta band power for high than low competition, which
26 mediated the impact of subsequent stimuli competition on behavioral performance. Overall, our
27 results show that, whereas preactivation of the internal templates associated with the category to
28 select are engaged in advance in both competition contexts, their underlying neural patterns
29 differ. In addition, these codes could not be associated with theta power, suggesting different
30 preparatory processes. The implications of these findings are crucial to increase our
31 understanding of the nature of top-down processes across different contexts.
32

33 **Keywords:** biased competition model; selective attention; MVPA; preparation; EEG

34 **1. Introduction**

35 In our everyday life we are surrounded by myriads of stimuli, but only some of them occupy our
36 mind. The process of selective attention relates to the filtering of unwanted information and the
37 selection of the pieces that are relevant to us. This intricate cognitive function proceeds through
38 various biasing routes: one involves bottom-up processes, where the characteristics of stimuli
39 automatically capture attention, while another is guided by goals, following top-down processes
40 (Desimone & Duncan, 1995). The latter does not only take place during stimulus processing but
41 can also happen in anticipatory fashion, by activating goal-related information before target
42 events. This preparatory selection is related to proactive cognition (Braver, 2012). However,
43 research about how such preparation unfolds to aid selection in contexts with different
44 attentional demands is scarce.

45 One of the most influential proposals explaining selective attention is the biased competition
46 model (Desimone & Duncan, 1995). This framework highlights the limited capacity of neural
47 information processing and the essential role of competition in resolving this problem. As we
48 move up along the cortical hierarchy, neurons increase their receptive fields to respond to
49 stimuli. However, given the limits of their response, the more pieces of information (e.g.,
50 objects) are placed in the same receptive field, the less information there will be about each of
51 them. Thus, neurons are selective and prioritize certain types of information, and thus the
52 information that reaches our senses competes to be represented. Such competition is biased by
53 bottom-up and top-down mechanisms. While bottom-up mechanisms may favor, for example,
54 the most salient stimulus, top-down processes engage neurons in the prefrontal cortex that
55 generate internal templates representing relevant information. These templates are used to bias
56 neural competition favoring goal-relevant information. For example, if we aim to recognize a
57 friend's face in a crowd, pre-activation of a template of that face would later guide the
58 attentional selection.

59 Early studies explored how top-down biases affect spatial selection (Moran & Desimone, 1985;
60 Richmond et al., 1983) during target processing. To do this, authors compared the neural
61 responses to stimuli in contexts of differential competition manipulated by the presence or
62 absence of distractors. The first insights were obtained from electrophysiological cell recordings
63 in non-human primates. For example, Moran and Desimone (1985) examined neurons of the
64 visual cortex in a spatial attention task where monkeys had to respond to target stimuli placed at
65 specific locations. They used stimuli with features that were effective or ineffective for a
66 particular cell response. When these stimuli were presented simultaneously in the receptive field
67 of the cell and the monkey attended to the effective stimulus, the neuron's response was
68 enhanced, whereas it was attenuated when the animal attended to the ineffective stimulus.
69 Therefore, the cell's response was determined by the properties of the attended stimulus. Later
70 on, these findings were supported by data in humans using functional magnetic resonance
71 imaging (fMRI). Kastner et al. (1998) studied how competition is resolved in the human brain
72 when multiple stimuli appear simultaneously (a high competition context) or sequentially (low
73 competition). They found that in conditions of inattention, a high competition context generated
74 less activity in the visual cortex compared to a sequential presentation, indicating suppression of
75 activation due to competition. Crucially, when the competition was biased by top-down spatial
76 attention, neural suppression was reduced, corroborating the idea that focused attention
77 magnifies attended information by mitigating the suppression caused by nearby stimuli. More
78 recent studies have shown that selection also results in a heightened representation of specific
79 characteristics of the attended stimuli (Kaiser et al., 2016; Reddy et al., 2009; Sheldon et al.,
80 2021). These findings have been possible thanks to the use of advanced analytic techniques such
81 as multivariate pattern analysis (MVPA), which has allowed to detect how brain activity
82 patterns encode templates of attended features (Jackson et al., 2017) or categories (Kaiser et al.,
83 2016; Reddy et al., 2009) of stimuli. Moreover, other studies have revealed changes in
84 oscillatory activity, especially on the theta band. An increase in theta power has been found in
85 midfrontal regions during target processing when conflictive stimuli compete with the target
86 (Chevalier et al., 2021; Nigbur et al., 2011, 2012). Overall, this literature shows how stimulus
87 selection in competition contexts is a complex process in which different neural mechanisms
88 take part.

89 The studies discussed so far did not address neural processes that may be engaged during the
90 preparation when the presence of upcoming competing stimuli can be anticipated. Some other
91 studies have focused on preparatory activity (González-García et al., 2016; Peelen & Kastner,
92 2011; Peñalver et al., 2023; Rajan et al., 2021) but did not explore how varying levels of
93 competition might influence specific preparatory processes. A fruitful approach to investigate
94 preparation uses anticipatory cues to track preparatory templates, aligning with the principles of

95 biased competition theory. This way, it has been found that both spatial and content-based
96 information is preactivated before the target presentation (Rajan et al., 2021). For example,
97 Peelen and Kastner (2011) used symbolic cues to instruct participants to detect either people or
98 cars on naturalistic images entailing high levels of competition. Using MVPA, they compared
99 the activity patterns in the visual cortex during the preparatory interval and during visual
100 processing of exemplars from the target categories. Their results showed shared neural codes
101 across both epochs, suggesting that an attentional template similar to the one guiding visual
102 processing was preactivated during the preparation, biasing the competition in favor of stimuli
103 matching this template. More studies have also found preparatory templates associated with
104 relevant target categories (González-García et al., 2016; Peñalver et al., 2023; Ruz & Nobre,
105 2008) or stimulus features (Stokes et al., 2009) to attend. In a complementary manner, time-
106 frequency analyses have revealed that theta power during the preparation period is associated
107 with anticipating most challenging tasks (Cooper et al., 2017; Van Driel et al., 2015). Moreover,
108 the behavioral relevance of both MVPA and time-frequency results has been evidenced by
109 showing how both indices correlate with performance. On one hand, previous studies have
110 shown a behavioral improvement when preparatory activity patterns associated with the target
111 are more segregable (González-García et al., 2017; Peelen & Kastner, 2011; Soon et al., 2013;
112 Stokes et al., 2009), when the dimensions to attend are better distinguished (Hall-McMaster et
113 al., 2019) or when the working-memory load of the task is better represented (Manelis & Reder,
114 2015). On the other hand, preparatory theta power in frontocentral electrodes has been related to
115 a more consistent behavior on task-switching paradigms (Cooper et al., 2017) or to a necessary
116 step to accurate fast responses (Formica et al., 2022). However, the relationship between
117 anticipated coding of specific information across contexts, theta power and behavioral
118 performance remains uncertain.

119 In this work we examined if and how preparatory neural signals (i.e., the presence of target-
120 specific activity patterns and theta band power increases) are affected by anticipated
121 competition levels, as well as the relationship among them and with task performance. To do so,
122 we collected EEG data during a cue-target paradigm with different levels of competition across
123 blocks, including a separate localizer task to isolate perceptual templates. We analyzed
124 anticipatory neural activity with univariate (time-frequency) and MVPA approaches.
125 Considering previous findings (Hall-McMaster et al., 2019; Manelis & Reder, 2015; Peelen &
126 Kastner, 2011; Peñalver et al., 2023), we expected that preparatory patterns would dissociate
127 based on the relevant target category, and that this category-specific pattern would be more
128 distinguishable in a high competition context. Also, at the oscillatory level we predicted that the
129 amplitude of preparatory theta power would be enhanced in high competition (Cooper et al.,
130 2017; Van Driel et al., 2015). Finally, we hypothesized that these preparatory brain signals
131 would be related to behavioral performance (Formica et al., 2022; González-García et al., 2017;
132 Peelen & Kastner, 2011; Soon et al., 2013; Stokes et al., 2009).

133 2. Methods

134 2.1. Participants

135 Thirty-six students (mean age = 21.36; range = 18-27; 18 women and 18 men) from the
136 University of Granada, all native Spanish speakers, right-handed and with normal or corrected
137 vision, were recruited and gave their informed consent to participate. They received 20-25 euros
138 depending on their task performance. We excluded three additional participants due to either
139 low accuracy (lower than 80%) or more than 30% discarded EEG trials due to artifacts. Data
140 were collected during the COVID-19 pandemic; therefore, participants' temperature was
141 measured upon arrival, they wore a face mask during the experiment and signed a form
142 confirming not having illness symptoms.

143

144 We calculated the sample size using PANGEA (Power ANalysis for GEneral ANOVA designs;
145 Westfall, 2016). Our task followed a 3-factor within-subjects design (Competition x Stimulus
146 Category x Congruency) where our main contrast of interest was a two-way interaction
147 (Competition x Congruency). To achieve an estimated 80% power to detect a small-medium
148 behavioral effect size of Cohen's $d = 0.3$, we required a minimum of 30 participants.
149 Nonetheless, to match counterbalancing needs we collected data from 36 participants, with an
150 estimated power of 87%.

151

152 **2.2. Apparatus, stimuli and procedure**

153 The task was run on Matlab 2020a using The Psychophysics Toolbox 3 (Brainard, 1997).
154 Stimuli were presented on an LCD screen (1920×1080 resolution, 60 Hz refresh rate) over a
155 grey background. We used four types of stimuli as cues: circle, square, drop and diamond with
156 thin black outlines, unfilled. As targets and distractor stimuli we employed 24 Caucasian faces
157 with neutral expressions from the Chicago Face Dataset (Ma et al., 2015) and 24 Spanish person
158 names (50% male-female in both categories).

159

160 When participants arrived to the lab they signed an informed consent, and then the EEG
161 preparation started. They read the instructions of the task and performed a practice session (192
162 trials identical to the main task), where they had to achieve 80% of accuracy on both High and
163 Low competition blocks to continue with the experimental session.

164

165 The experiment consisted of two tasks presented on different blocks: a main competition task
166 and a stimulus category localizer. The main task was a cue-target paradigm where participants
167 judged the sex of target faces and words. Cues presented at the beginning of each trial indicated
168 the category of the target (faces/names) to respond to. Target and distractors were displayed
169 either simultaneously (in High competition blocks, 50%) or sequentially, with a temporal delay
170 (Low competition, 50%; adapted from Kastner and colleagues, 1998). Target and distractor
171 stimuli could be either congruent (i.e., same sex, associated with the same response, 50%) or
172 incongruent (different sex, with different responses, 50%). At the beginning of each block, an
173 instruction screen stated the level of competition (High vs. Low) and indicated the cue-target
174 associations for the block. To prevent perceptual confounds in the multivariate analyses, each
175 category (faces and words) was cued with two different stimuli for each participant. That is, two
176 cues always indicated faces, and the other two names. One of each pair was used in each block
177 (one for faces and another one for names). Within participants, we counterbalanced the
178 combination of cues across blocks, sequentially iterating across all possible pairs of face and
179 name cues. The association between cues and target categories was further counterbalanced
180 across participants.

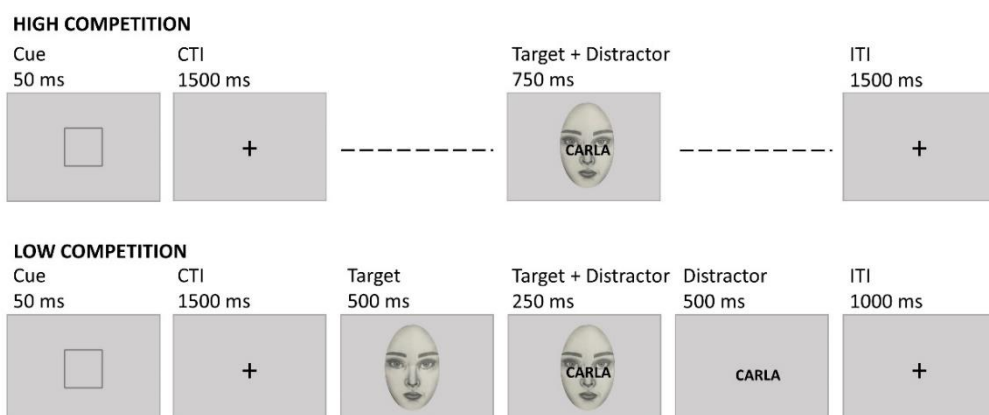
181

182 The sequence of events in a trial was as follows (see Figure 1): The cue ($\sim 2^\circ \times 2^\circ$ degrees of
183 visual angle) was presented for 50 ms and was followed by a Cue-Target-Interval (CTI) of 1500
184 ms. In High competition blocks, an overlapping face ($\sim 9.7^\circ \times 12.17^\circ$ visual angle) and a name
185 ($\sim 9.7^\circ \times 2.6^\circ$ visual angle) used as target and distractor stimuli were displayed for 750 ms,
186 followed by an Inter-Trial-Interval (ITI) of 1500 ms. In Low competition blocks, the target
187 appeared first on the screen for 500 ms, followed by overlapping target and distractor for 250
188 ms and then by the distractor on its own for 500 ms, ending with a 1000 ITI ms. This
189 arrangement follows previous similar paradigms (see Kastner et al., 1998) and allows to present
190 each stimulus with the same duration and maintain the same trial length across competition
191 conditions. The response window was the same in both conditions. Participants pressed the keys
192 "A" or "L" with their left and right index to indicate whether the target stimulus was female or

193 male (counterbalanced across participants). In case of wrong answers, after the ITI, a feedback
194 tone of 450 Hz was played for 300 ms while a fixation cross was displayed for 1000 ms in total.
195

196 In Localizer blocks, included to isolate the perceptual processing of stimuli without motor
197 activity, the same faces and names were presented for 750 ms followed by an ITI of 500 ms. To
198 facilitate participants' engagement with the task, they were instructed to press the "C" key in a
199 minimal percentage of trials (8%) where the target was rotated 180°.
200

201 There were 72 blocks, 24 of each type (High competition, Low competition and Localizer). The
202 order of blocks was fully counterbalanced within and across participants, as each block was
203 preceded and followed by the other types the same number of times. For the main task, we had
204 576 trials for each (High, Low) competition condition. These trials were unique combinations of
205 the 24 faces and 24 names. Each block lasted 1.52 minutes (with 24 trials of 3.8 s each). The
206 localizer blocks had 48 trials lasting 1.25 s, for a total of 1 minute per block (for a total of 1152
207 localizer trials). The whole session, including practice, lasted approximately 2 hours and 15
208 minutes.



209

210 **Fig. 1.** Experimental paradigm. Example trials from High and Low competition blocks. In a sex
211 classification task, participants were cued about which stimulus category (faces or names) to
212 respond to. In High competition blocks, targets and distractors appeared at the same time,
213 whereas in Low competition they appeared sequentially.
214

215 **2.3. EEG acquisition and preprocessing**

216 EEG data was recorded with a high-density 64 active channels cap (actiCap Slim, BrainVision)
217 at the Mind, Brain and Behavior Research Center (CIMCYC) of the University of Granada. The
218 impedances of the amplifier were kept below 10 k Ω. EEG activity was recorded at a sampling
219 rate of 1000 Hz, with FCz as the reference electrode.
220

221 Preprocessing was done using EEGLAB (Delorme & Makeig, 2004) and in-house MATLAB
222 scripts following the pipeline available on Github (see Open practices section). First, data were
223 downsampled to 256 Hz and filtered using a low-pass and high-pass FIR at 120 and 0.1 Hz,
224 respectively. A notch filter was applied at 50 and 100 Hz to remove line noise and its
225 harmonics. Noisy channels were identified by visual inspection and removed (1 channel on
226 average, range 0-4). Next, the data was epoched in intervals of 3 s (-1 to 2 s after the onset of
227 cues and of targets). Independent Component Analysis (ICA) was computed afterwards with the
228 runica algorithm from EEGLAB to remove blinks and lateral eye movements. Components

were selected with ICLabel and visual inspection (scalp maps, raw activity and power spectrum). An average of 1.58 components per participant (range 1-3) were removed. Then, automatic trial rejection was used to prune the data from other artifacts, using 3 criteria (see López-García et al. (2020, 2022) and Peñalver et al. (2023) for similar parameters). First, we identified trials with abnormal spectra, removing those deviating from baseline by ± 50 dB in the 0–2 Hz frequency window (sensitive to remaining eye artifacts) or by -100 dB or +25 dB in 20–40 Hz (sensitive to muscle activity). Second, trials with improbable data were eliminated: the probability of occurrence of each trial was computed by determining the probability distribution of voltage values across trials, with a rejection threshold established at ± 6 SD. The third criteria were extreme values: all trials with amplitudes in any electrode out of a ± 150 μ V range were rejected. Next, the dismissed channels were recomputed by spherical interpolation and a common average was used to re-reference the data. Finally, we applied a baseline correction in the -200 to 0 ms prior to stimulus onset. The analyses focused solely on correct trials. On average, 1476 trials per participant (range 1292-1591) were included.

243

244 2.4. Analyses

245 2.4.1. Behavioral

246 We employed 2-way repeated measures ANOVAs with the factors Competition (High vs. Low) 247 and Congruency (Congruent vs. Incongruent). Separate tests were performed on accuracy and 248 reaction times (RT) using the JASP software (Love et al., 2019). To filter the RT data, we 249 excluded incorrect trials and those with RT deviating 2SD from the participant mean.

250

251 2.4.2. EEG

252 2.4.2.1. Multivariate pattern analysis (MVPA)

253 We used Linear Discriminant Analyses (LDA) as classifiers to investigate if the preparatory 254 activity patterns contained information about the upcoming competition level (High or Low) 255 and the specific target categories (Faces or Names) anticipated across competition contexts. To 256 do so, we focused on the cue-locked interval activity from -100 to 1550 ms. The analyses were 257 run on MATLAB using the toolbox MVPAlab (López-García et al., 2022). Classifiers were 258 trained and tested using raw voltage of each trial and time point across all the channels, with the 259 configuration for the classification being equal for all the analyses.

260

261 To increase the signal-to-noise ratio, we created ‘supertrials’ (Grootswagers et al., 2017) by 262 averaging three random trials within each condition (see López-García et al. (2020, 2022); 263 Peñalver et al. (2023) for similar procedures) and smoothed the data by applying a moving 264 average window every three time points, so that data from every timebin (t_n) was averaged with 265 the previous and the following time-points $t_n = (t_{n-1} + t_n + t_{n+1})/3$. We used a 5-fold cross- 266 validation strategy that ensures unbiased results while reducing the computational cost 267 (Grootswagers et al., 2017). With this approach, we split our data into five subsets and used four 268 to train the classifier and the remaining one as a test set. This protocol was repeated 5 times, 269 changing the test set. The number of trials within each class was subsampled considering two 270 criteria: that each class had the same number of trials and that there was the same number of 271 trials per class in each fold for the cross-validation procedure (Grootswagers et al., 2017; King 272 & Dehaene, 2014). A normalization procedure was applied to enhance the classifier 273 performance and generalizability of the results. Normalization was done during the cross- 274 validation, by calculating the mean and standard deviation of each electrode within each fold 275 across the training trials, and then applying these two values to normalize the data of both the 276 train and the test set as:

$$277 X_{\text{train}} = (X_{\text{train}} - \mu_{\text{train}}) / \sigma_{\text{train}} \quad X_{\text{test}} = (X_{\text{test}} - \mu_{\text{train}}) / \sigma_{\text{train}}$$

278

279 Where μ_{train} is the mean and σ_{train} is the standard deviation of the training set. Finally, to reduce
280 the computational cost, the analysis was done every three time points. The results are reported
281 as the area under the curve (AUC), a non-parametric criterion-free method with no assumptions
282 about the true distribution of the data (King & Dehaene, 2014). Also, AUC is sensitive to binary
283 (two-class) differences, less vulnerable to biases (including those triggered by potential
284 differences between the classes) and can be interpreted as classification accuracy (King et al.,
285 2013).

286

287 To detect the significant decoding performance at the group level, we used a non-parametric
288 cluster-based permutation method against empirical chance. For this, the trial labels were
289 randomly permuted 100 times per participant, resulting in chance-level outcomes under the null
290 effect. After that, one random AUC per participant was selected and averaged to create a group-
291 level null effect decoding curve. This was done 10^5 times to generate 10^5 permuted group AUC
292 values. These values were used to build empirical chance-level AUC distributions for each time
293 point. The AUC values in the 95 percentiles were used as threshold to identify significant
294 decoding peaks in the real decoding results. Moreover, to estimate the minimum cluster size to
295 be significant ($\alpha = 0.05$), we used the permuted results to generate a null distribution of cluster
296 sizes and corrected for multiple comparisons using a False Discovery Rate (FDR) approach
297 (López-García et al., 2022).

298

299 Additionally, we studied the extent to which the activity patterns were stable along the
300 preparation interval. For that purpose, we used a temporal generalization approach that applied
301 the decoding analysis explained above but training in a given time point and testing in all the
302 remaining ones. This procedure iterated using all time points as training and testing datasets.
303 This resulted in a Temporal Generalization Matrix with a diagonal reflecting the same result as
304 the MVPA curve and non-diagonal values corresponding to the temporal generalization of the
305 underlying neural code. The statistical significance from these matrices was extracted with the
306 same cluster-based analysis as before, now considering two-dimensional clusters that spread
307 over training and testing time points.

308

309 With this overall approach, we first studied if the competition level affected preparatory
310 activity. To do so, we trained and tested classifiers on the cue-locked interval of trials from
311 High and Low competition blocks. Then, to evaluate whether and how the preparatory interval
312 carried information about the target category anticipated, either faces or names, we performed
313 classification analyses separately for High and Low competition blocks. To compare the
314 category-related patterns while avoiding perceptual confounds triggered by the specific shape of
315 the cues, we adopted a cross-classification approach (Kaplan et al., 2015; Peñalver et al., 2023).
316 The classifiers decoding the relevant category were trained and tested in trials where
317 independent sets of cues were employed. This protocol iterated across the two sides of the
318 classification (exchanging training and testing cues) and all cues' combinations (e.g.: circle-
319 names, diamonds-faces vs. drops-names, squares-faces). Results were averaged across
320 directions and classifiers.

321

322 Additionally, we further studied if category-specific coding was affected by the competition
323 level anticipated in High and Low competition contexts, following two approaches. First, we
324 tested the hypothesis that preparing for high competition contexts increased the fidelity of
325 anticipatory category-specific neural codes. To do this, we compared the two competitions
326 cross-decoding curves and temporal generalization matrices using a tailored cluster-based
327 permutation approach (Moore et al., 2024). We computed one-tailed t -tests in every time point
328 to address whether the decoding accuracy or the temporal generalization was higher in High

329 than Low competition contexts. Then, we identified cluster sizes in these results, by looking for
330 sets of temporally adjacent points with $p < 0.05$. For that purpose, we set a criterion of a
331 minimum cluster size of 3 time points the cross-decoding curve, and 10 for temporal
332 generalization (Peñalver, 2024). To each of these clusters, we assigned a t value resulting from
333 the sum of the t values from all the time points incorporated. Next, the inference was performed
334 contrasting these results against a permutation-based distribution of null differences. To do so,
335 we randomly multiplied one of the conditions by -1 in each subject; this was done 5000 times.
336 We repeated the procedure as in the true data but with the permuted results, obtaining a
337 distribution of the t values of the clusters, and used the 95th percentile to mark the values that
338 were considered significant in the true data. Second, to further explore whether the competition
339 context altered the neural codes underlying the anticipatory category patterns, we performed a
340 cross-classification training and testing the classifier with data from different competition
341 blocks (Kaplan et al., 2015). This analysis also implemented the cross-classification across cues,
342 following a similar approach as above. The AUC curves obtained were averaged among
343 classifiers and directions.

344

345 To study whether the preparatory activity patterns associated with categorical information of
346 faces and names were similar to the actual perception of the stimuli, we performed a cross-
347 classification analysis by training with data from the localizer blocks and testing on the cue-
348 locked window of the main task, separately for High and Low competition. As the timing of the
349 localizer and main task paradigm were different, we focused on the temporal generalization
350 profile of the cross-classification. Considering that our interest was the reinstatement of
351 perceptual patterns on preparation activity, this cross-classification was only performed in a
352 single direction, using the localizer data as training set and the main task data as test set. To test
353 whether the reinstatement has different robustness in High or Low-competition contexts, we
354 compared these matrices using two-tailed t -tests with a cluster-based permutations approach.
355 This analysis was equivalent to the one comparing the category-specific coding across
356 competition conditions, except for using two-tailed tests.

357

358 Finally, to study the link between anticipatory activity patterns and task performance, decoding
359 results and behavioral data were correlated using the Pearson coefficient. First, we used the
360 anticipated competition level, extracting the average AUC value for each participant during the
361 time window where the decoding was significant at the group level, from 100 ms until the end
362 of the interval (see Li et al., 2022). This value was correlated with behavioral accuracy and RT
363 means across High and Low competition. To check for specific relationships between the
364 congruency behavioral effect and the anticipated competition level, we calculated differences in
365 task performance (separately for behavioral accuracy and RT) of congruent minus incongruent
366 trials and correlated this with individual AUC values. Second, we followed a similar strategy
367 with the fidelity of the category-specific decoding, but in this case, the AUC values of each
368 participant were calculated separately for High and Low competition blocks. We averaged the
369 AUC values during the time window that was significant in both High and Low competition
370 contexts (1150-1550 ms). Then, we correlated the AUC with the behavioral accuracy and RT of
371 each competition condition. To address the relationship with the congruency effect, we
372 calculated the difference between the congruent and incongruent trials of each competition
373 condition separately and correlated them with the mean AUC values of each condition. In all
374 cases, we applied frequentist and Bayesian statistics to provide complementary evidence
375 supporting the results.

376

377 **2.4.2.2. Time-frequency analysis**

378 We tested whether preparing for High competition increased anticipatory theta-band activity (3-
379 7 Hz) in comparison with Low competition. Theta power was extracted from a frontocentral
380 region of interest (ROI) with the electrodes Fz, FC1, Cz, FC2, F1, C1, C2, F2 and FCz. We
381 computed the time-frequency decomposition for each trial during the preparation epoch (cue
382 locked -1000 to 1550 ms) using complex Morlet wavelets. The frequencies were logarithmically
383 spaced in 18 steps from 2 to 20 Hz. The wavelet's length was calculated separately for each
384 frequency assigning a number of cycles also logarithmically spaced between 3 and 5 (see
385 Cohen, 2019). Time-frequency power values were transformed to decibels and normalized to a
386 baseline of -280 to -100 ms before cue onset, according to the following equation (Cohen &
387 Van Gaal, 2014): $dB = 10 * \log_{10}(\text{power}/\text{baseline})$.

388
389 A cluster-based nonparametric statistical test implemented in FieldTrip (Maris & Oostenveld,
390 2007) was used to evaluate whether the preparatory activity of High competition trials showed
391 higher theta power than Low competition ones. For this, power values in each condition were
392 averaged across channels and trials. Then, these averages were compared using within-subjects
393 paired-samples two-tailed *t*-test for each time point and frequency (Hz). Those *t* values larger
394 than the threshold specified by alpha (0.05) were clustered in connected sets of temporal
395 adjacency. The *t* value of the cluster was calculated adding the *t* values of each timepoint. The
396 permutations were performed within each subject randomizing the condition labels for each
397 value, 1000 times with the Monte Carlo method. *T* values were calculated for all the
398 permutations using maximum cluster-level mass statistic (Groppe et al., 2011), and the most
399 extreme cluster-level *t* score across permutations was used to derive a null hypothesis
400 distribution. If the *t* value of the true data cluster was above the 97.5th percentile or below the
401 2.5th percentile of the null distribution, then it was considered significant.

402
403 Next, to explore whether anticipatory theta power increase and the content-specific activity
404 patterns found with the decoding were related, we correlated them using Pearson across
405 participants, separately for High and Low competition conditions. To obtain the theta power
406 values per participant, we visually inspected the grand average across trials from all conditions
407 and identified the theta time window from 100 ms to 900 ms (see Fig S1). We extracted the
408 average theta amplitude per participant from this time window. Then, these values were
409 correlated with the classification AUC per participant and competition condition averaged
410 within the 1150 ms to 1550 ms time window.

411
412 Finally, we performed a mediation analysis to investigate if the anticipatory theta power acted
413 as a mediator between the competition manipulation and the speed of responses (e.g., Formica
414 et al., 2022). To do so, we used trial-by-trial RT and theta power data, averaging the power
415 values within 100-900 ms after cue presentation (same time window as above). To filter out
416 outlier data, trials with $\pm 2SD$ from the average RT or theta power were discarded. Afterwards,
417 we verified that the data fitted the necessary criteria (Baron & Kenny, 1986) for mediation
418 analysis: in our case (1) the competition manipulation had to influence RTs, (2) this
419 manipulation also had to predict theta power, and (3) theta power had to predict RTs. These
420 were tested with linear mixed effects models (LMMs) with the lme4 package in R (Bates et al.,
421 2014). In all models, we included Congruency as a fixed effect to control for it. To select the
422 model with an adequate random effect structure, a “keep it maximal” approach was adopted
423 starting with the most complex random structure until the model converges for the 3 LMMs
424 (Barr et al., 2013). This approach gave a random structure of (competition | subject). P-values
425 were calculated using Satterthwaite approximations (Luke, 2017). Once we ensured the three
426 criteria were met, the mediation was tested performing a causal mediation analysis with the

427 function mediate from the mediation package in R, using 5000 permutations (Tingley et al.,
428 2014).

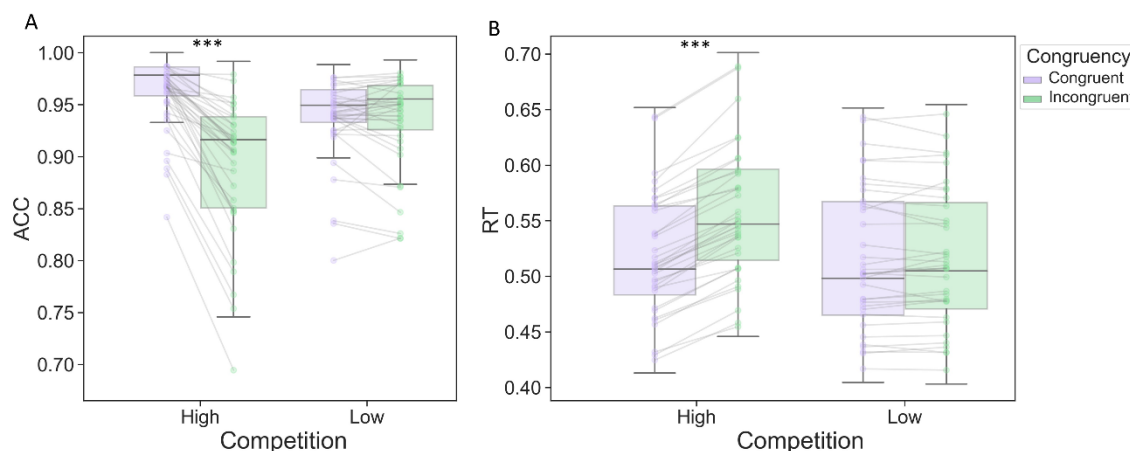
429 **3. Results**

430 **3.1. Behavioral**

431 Overall accuracy on the main task was 93.5%. The ANOVA of accuracy data showed a main
432 effect of Competition ($F_{35,1} = 16.022, p < 0.001, \eta_p^2 = 0.314$), indicating that participants
433 performed better on Low ($M = 93.8\%, SD = 4.4\%$) than High competition blocks ($M = 92.3\%,$
434 $SD = 5.2\%$). The Congruency effect ($F_{35,1} = 71.269, p < 0.001, \eta_p^2 = 0.671$) was also significant,
435 showing that Congruent trials were more accurate ($M = 95.1\%, SD = 3.8\%$) than Incongruent
436 ones ($M = 91.2\%, SD = 5.8\%$). As predicted, there was a significant interaction of Congruency
437 * Competition ($F_{35,1} = 73.030, p < 0.001, \eta_p^2 = 0.676$). Post-hoc test showed that the
438 Congruency effect appeared in High ($M_{\text{Congr}} = 95.9\%, M_{\text{Incongr}} = 88.6\%, t_{35,1} = 9.319, p < 0.001,$
439 Cohen's $d = 1.553$) but not in Low competition ($M_{\text{Congr}} = 94.1\%, M_{\text{Incongr}} = 93.6\%, t_{35,1} = 1.555,$
440 $p = 0.129$, Cohen's $d = 0.259$).

441 An average of 5.5% trials per participant, corresponding to outliers' values of RT ($\pm 2SD$), were
442 excluded. The ANOVA results showed a main effect of Competition ($F_{35,1} = 26.664, p < 0.001,$
443 $\eta_p^2 = 0.432$), as participants were slower on High ($M = 535.0 \text{ ms}, SD = 60.0$) compared to Low
444 competition trials ($M = 514.0 \text{ ms}, SD = 68 \text{ ms}$). There was also an effect of Congruency ($F_{35,1} =$
445 $224.819, p < 0.001, \eta_p^2 = 0.865$) with faster Congruent ($M = 515.0 \text{ ms}, SD = 62.0$) than
446 Incongruent ($M = 534.0 \text{ ms}, SD = 63.0$) trials, and an interaction of Congruency * Competition
447 ($F_{35,1} = 203.907, p < 0.001, \eta_p^2 = 0.853$). Again, Congruency was only present in High
448 competition ($M_{\text{Congr}} = 517.0 \text{ ms}, M_{\text{Incongr}} = 556.0 \text{ ms}, t_{35,1} = -19.021, p < 0.001$, Cohen's $d = -$
449 3.170) and not in Low competition blocks ($M_{\text{Congr}} = 514.0 \text{ ms}, M_{\text{Incongr}} = 514.0 \text{ ms}, t_{35,1} = 0.065,$
450 $p = 0.949$, Cohen's $d = 0.011$).

451



452
453 **Fig. 2.** Box plots displaying the behavioral results. Boxes have a middle marking the median,
454 limits representing the first and third quartile, and whiskers indicating the 1.5 inter quartile
455 range for the upper and lower quartiles. Outliers are shown outside the whiskers. The dots
456 represent each participant's value per experimental condition. (A) Behavioral accuracy rate
457 (ACC) in High and Low competition blocks for Congruent and Incongruent trials. (B) Reaction
458 times (RT in seconds) in High and Low competition blocks for congruent and incongruent trials.
459 *** = $p < 0.001$

460

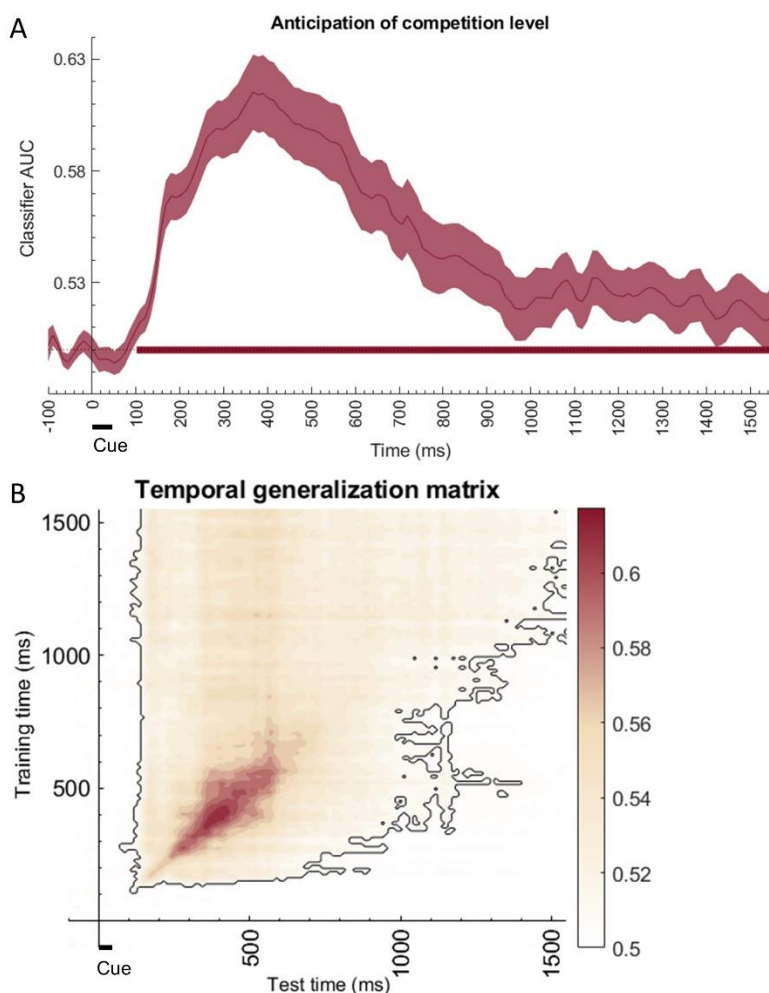
461

462 **3.2. Electrophysiology**

463 **3.2.1. MVPA results**

464 **3.2.1.1. Anticipation of the competition level**

465 Our first aim was to assess the anticipation of the overall competition level. A classifier trained
466 and tested to discriminate preparatory activity between High and Low competition contexts
467 showed an effect of competition. The cluster identified in these results covered most of the CTI
468 (from 100 ms until the end of the interval, see Fig. 3A). The temporal generalization analysis
469 revealed a large significant cluster starting approximately at 100 ms. Interestingly, the cluster
470 was asymmetric, generalizing to all the testing time points when the classifier was trained using
471 data from the end of the preparation window, whereas less generalization was found when the
472 training was done at the beginning of the interval (see Fig. 3B).

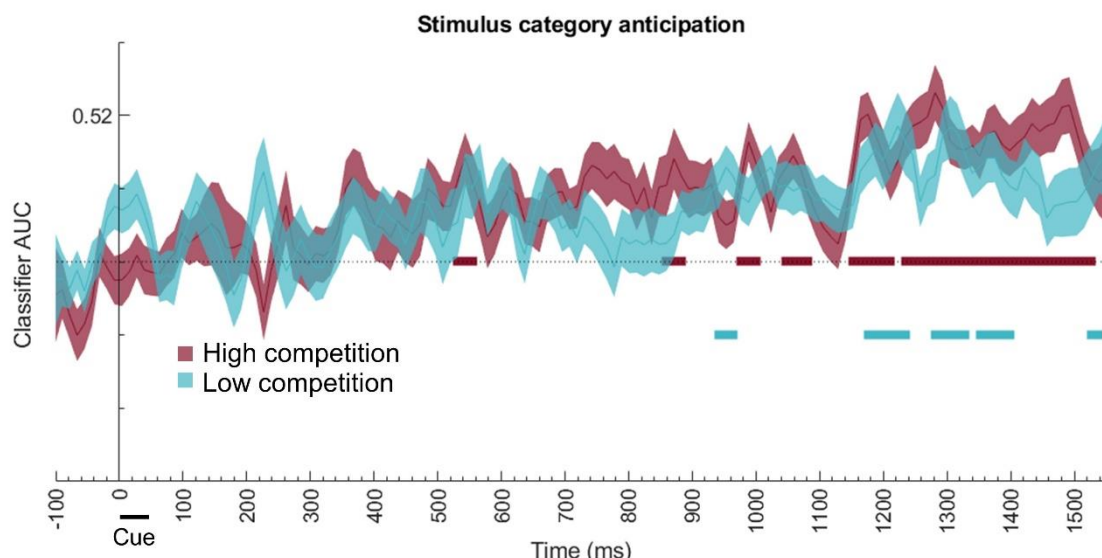


473

474 **Fig. 3.** (A) Classifier performance distinguishing competition levels in the preparation interval.
475 The red line shows the mean AUC and the shaded red areas its standard error. The red
476 horizontal line displays significant time points. The black horizontal line shows the onset and
477 duration of the cue. (B) Temporal generalization matrix from the same classification showing
478 significant above-chance clusters outlined in black. The color range in the bar indicates the
479 AUC values.

480

481 **3.2.1.2. Category-specific anticipation**
482 Classifiers trained and tested to discriminate the target category that the participants were
483 preparing to attend (faces vs. names) indicated that there was a significant effect of category.
484 We found decoding clusters in High (from 531-555 ms, 859-906 ms, 976-1000 ms, 1047-1082
485 ms, 1152-1211 ms, 1234-1527 ms) and Low competition contexts (941-965 ms; 1176-1234 ms;
486 1281-1328 ms; 1352-1398 ms; 1527-1550 ms). The decoding AUC incremented progressively
487 with a ramping up profile towards the end of the preparation interval, before target onset (see
488 Fig 4). Nonetheless, there was no evidence supporting different decoding accuracies across
489 competition conditions (all $p > 0.05$).

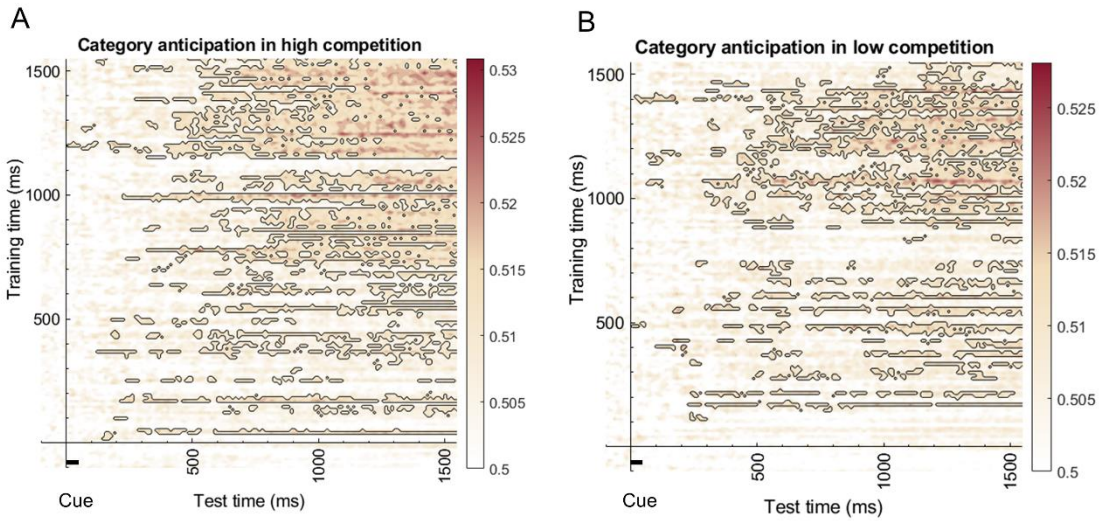


490

491 **Fig. 4.** Results (AUC values) of the classifiers discriminating the upcoming target category
 492 (faces vs. names) using cross-classification (across cues identities), separately for High and Low
 493 competition conditions. Horizontal lines represent the significant clusters for High (red) and
 494 Low (blue) competition.

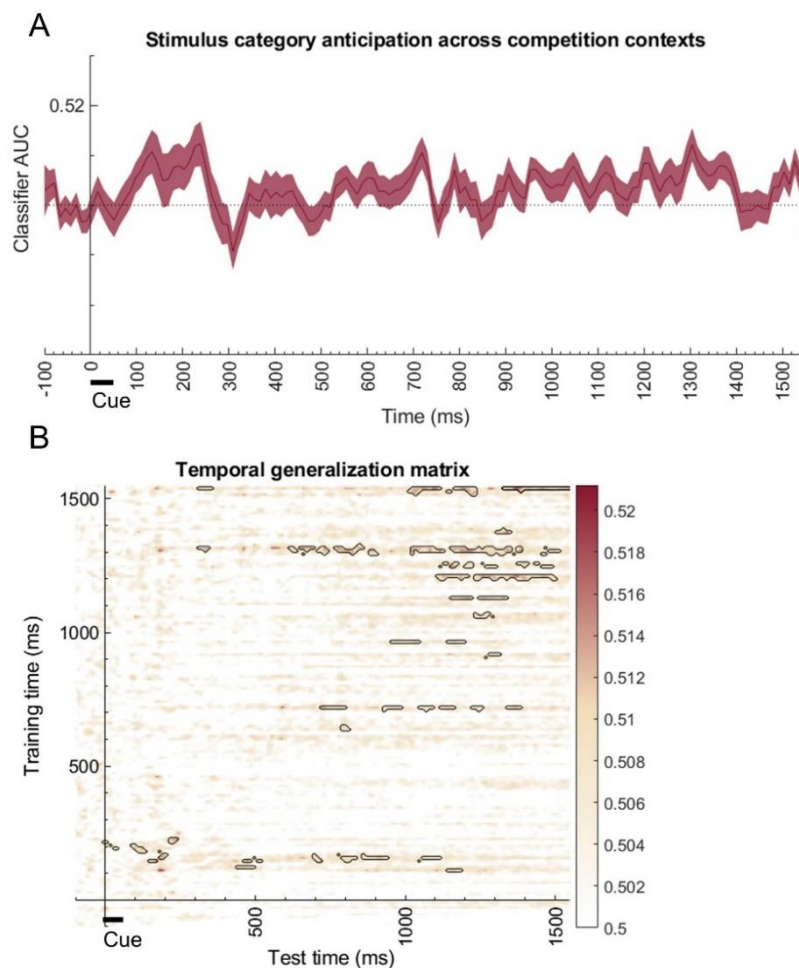
495

496 We also analyzed the temporal generalization of category-specific information separately for
497 High and Low competition contexts. For both, the anticipatory patterns showed temporal
498 generalization, which was stronger on the right upper corner of the matrix, towards the end of
499 the interval (Fig. 5). However, the comparison of both matrices did not provide statistical
500 evidence supporting different generalization patterns (all $ps > 0.05$).



501
502 **Fig. 5.** Time-generalization matrices of the discrimination of the upcoming target category
503 (faces vs. names) using cross-classification (across cues identities) on High (A) and Low
504 competition (B). Significant clusters above chance are outlined with black. The color range in
505 the bar represents AUC values.

506
507 We also tested whether these patterns in High and Low competition are coded similarly. A
508 cross-classification strategy across conditions and cues showed no evidence for similar patterns
509 coding the relevant category between competition contexts (Fig. 6A). The temporal
510 generalization analysis only showed small scattered significant clusters (see Fig. 6B).



511

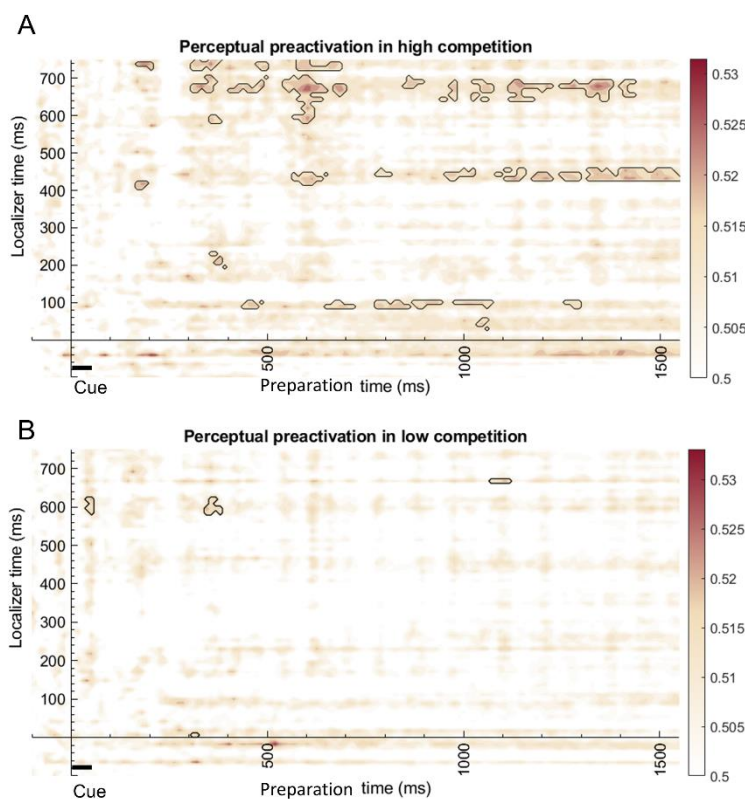
512 **Fig. 6.** (A) Cross-classification across competition conditions and cues differentiating upcoming
513 target categories, showing no significant clusters. (B) Temporal generalization matrix for the
514 same cross-classification showing small clusters above chance, outlined with black. The color
515 range represents AUC values.

516

517 3.2.1.3. Preactivation of perceptual patterns during preparation

518 Classifiers were trained to discriminate between faces and names in the localizer and tested
519 during the preparation interval of the main tasks separately for High and Low competition
520 contexts. The results showed several above-chance significant clusters in the High competition
521 context (Fig. 7A). In the preparation interval of Low competition trials, there were few above-
522 chance clusters (Fig. 7B). However, when comparing both matrices, there was no statistical
523 evidence supporting different preactivations of perceptual patterns across competition
524 conditions (all $p > 0.05$).

525



526
527 **Fig. 7.** Temporal generalization of the cross-classification from the localizer category targets to
528 the upcoming category targets in the preparation interval of (A) High competition and (B) Low
529 competition (with cue duration presented as the black horizontal line). The color range in the bar
530 represents AUC values.

531 3.2.1.4. Decoding-behavior relationships

532 To study whether the observed preparatory patterns of competition were related to behavioral
533 performance, we correlated the decoding accuracy of the classifier with the average accuracy
534 and RT across participants. However, Pearson correlations resulted in non-significant results (all
535 $ps > 0.6$). A Bayesian approach provided moderate evidence in favor of the null hypothesis, i.e.,
536 the absence of a relationship between the two variables (Mean behavioral accuracy: $r = 0.03$, p
537 = 0.87, $BF_{01} = 4.75$; Mean RT: $r = 0.09$, $p = 0.60$, $BF_{01} = 4.22$). We also correlated the
538 behavioral congruency effect (i.e., the accuracy and RT difference of congruent minus
539 incongruent trials) and the anticipation of competition level decoding. Pearson correlations were
540 non-significant (all $ps > 0.4$) and Bayesian factors showed moderated evidence towards the null
541 hypothesis (Behavioral accuracy: $r = -0.03$, $p = 0.83$, $BF_{01} = 4.71$; RT: $r = 0.11$, $p = 0.52$, $BF_{01} =$
542 3.94).

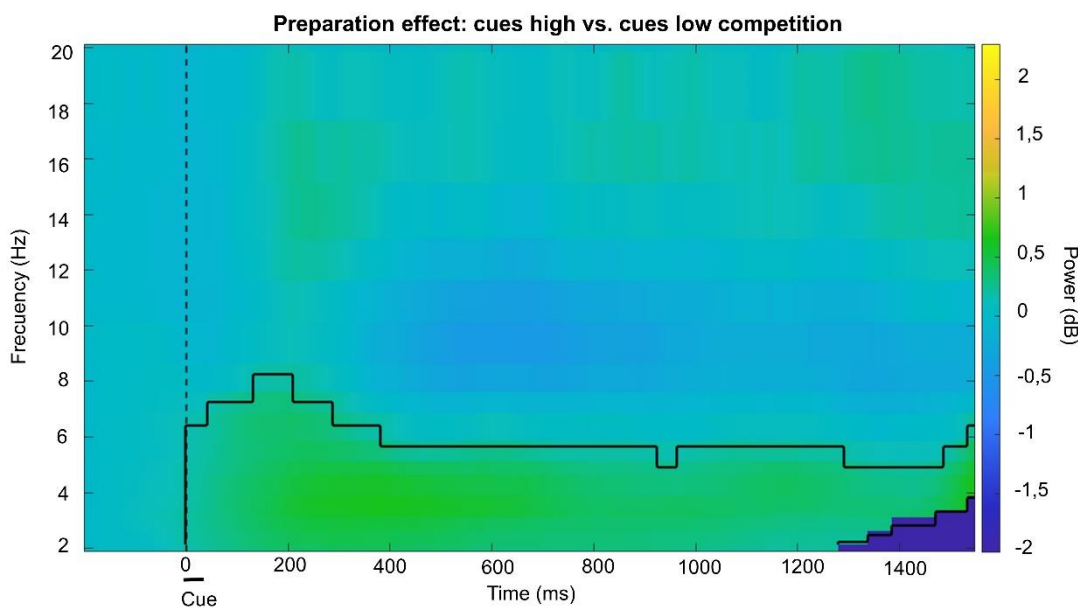
543
544 We also correlated behavioral performance with category-specific decoding values separately
545 for High and Low competition indexes. In this case, for each participant, we averaged the AUC
546 in the same time window for High and Low competition. Again, the Pearson correlations were
547 non-significant (all $ps > 0.2$) and Bayesian factors showed weak to moderate evidence in favor
548 of the null hypothesis (High competition accuracy: $r = 0.16$, $p = 0.34$, $BF_{01} = 3.12$; High
549 competition RT: $r = -0.22$, $p = 0.20$, $BF_{01} = 2.15$; Low competition accuracy: $r = -0.01$, $p =$
550 0.96, $BF_{01} = 4.81$; Low competition RT: $r = -0.01$, $p = 0.97$, $BF_{01} = 4.82$). A similar approach
551 was taken to correlate the congruency effect with the category-specific anticipation decoding.
552 The results indicated that none of the correlations were significant (all $ps > 0.2$), providing weak
553 to moderate evidence in favor of the null hypothesis (High competition, accuracy: $r = -0.03$, $p =$

555 0.88, $BF_{01} = 4.76$; High competition, RT: $r = 0.19, p = 0.27, BF_{01} = 2.68$; Low competition,
556 accuracy: $r = 0.03, p = 0.86, BF_{01} = 4.75$; Low competition, RT: $r < 0.01, p = 0.98, BF_{01} =$
557 4.82).

558

559 3.2.2. Time-frequency results

560 The comparison of the two conditions' time-frequency maps in the cue-locked interval showed
561 that High competition anticipation generated higher Theta power than Low competition. A large
562 cluster ($p < 0.001$, Fig. 8) was found around the Theta band (3-7 Hz) from 0 to 1550 ms.

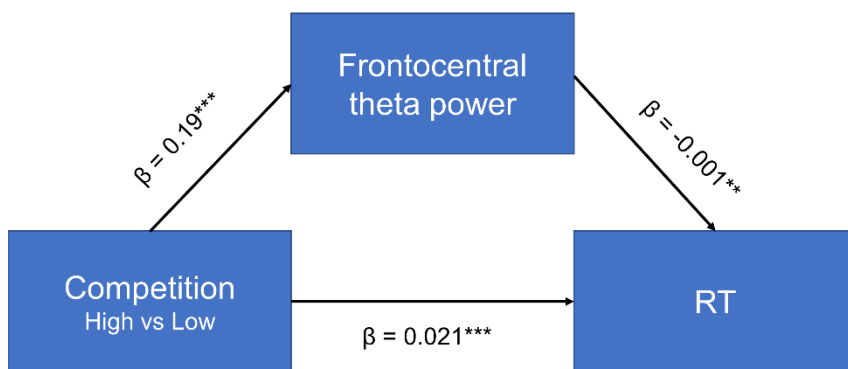


564 **Fig. 8.** Results of the Monte Carlo cluster-based approach comparing the power values of High
565 and Low competition trials during the preparation interval. The significant cluster is outlined
566 with black lines. The dark blue patch on the lower-right corner reflects the lack of estimated
567 power data due to edge effects.

568 The Pearson correlations between category-specific decoding and theta power in High and Low
569 anticipation conditions resulted in non-significant results (all $p > 0.6$). A Bayesian approach
570 provided moderate evidence supporting the null hypothesis (High competition: $r = 0.08, p =$
571 0.65, $BF_{01} = 4.37$; Low competition: $r = 0.08, p = 0.65, BF_{01} = 4.38$).

572

573 Finally, we explored whether the neural mechanisms reflected by the frontocentral theta power
574 could act as mediators between the impact of competition levels and the RTs. The filtering
575 performed prior to the analysis removed an average of 7.5% (SD = 1%) of trials for each
576 participant. We confirmed that our data met the necessary criteria for the mediation (Baron &
577 Kenny, 1986), fitting our data on three LMMs (see Supplementary materials for details). First,
578 in agreement with previous analysis, there was a Competition and Congruency effect on RTs.
579 Second, the effect of Competition on theta was also significant, so that High competition
580 induced higher theta power. Third, in the complete model predicting RTs there was an effect of
581 Congruency, Competition and also theta on RTs, suggesting that larger theta values were
582 associated with faster responses. To directly test that theta power partially mediates the effect of
583 competition on RTs, we performed a causal mediation analysis that showed a significant direct
584 effect of competition on RTs ($\beta = 0.022, CI 95\% = [0.013, 0.03], p < 0.001$) and an indirect
585 effect via theta ($\beta = -0.0001, CI 95\% = [-0.0002, 0], p = 0.006$), indicating a partial mediation
586 (see Fig. 9).



587

588 **Fig. 9.** Mediation model with beta values. The anticipated competition significantly predicted
589 frontocentral theta power, which in turn affected the RTs. Frontocentral theta power mediated
590 the effect of competition on RT, although the direct effect of competition on RT was still
591 significant after accounting for the mediating effect of theta, suggesting a partial mediation.
592 *** $p < 0.001$ ** $p < 0.01$

593 4. Discussion

594 In this study we examined how the anticipated demands of attentional selection, manipulated
595 through competition between target and distractors, modulated specific markers of preparatory
596 neural activity. In line with the postulates of the biased competition model, our results reveal the
597 preactivation of internal templates associated with the category to select. However, these
598 preactivations did not differ in robustness across competition contexts, and they did not
599 generalize between competition contexts, suggesting the existence of differential preparation
600 formats. Moreover, oscillatory activity showed higher theta band activity for high than low
601 competition context, an effect that mediates behavioral improvements.

602 Our behavioral results validated the effectiveness of the paradigm. The high accuracy rates
603 across conditions show that participants paid attention to the cues, and the congruency effect
604 was present only in the high competition condition, in line with classic studies (Beck & Kastner,
605 2009; Desimone & Duncan, 1995; Eriksen & Eriksen, 1974; Simon, 1969). The higher selective
606 attention demands were also reflected in lower accuracy and higher response times in the high
607 competition blocks, as expected (Desimone & Duncan, 1995; Duncan, 1993).

608 Multivariate classifiers showed that anticipated competition levels could be distinguished. These
609 differences between high and low competition contexts are in line with previous studies that
610 found evidence of preparatory coding of different tasks (González-García et al., 2017; Hall-
611 McMaster et al., 2019; Manelis & Reder, 2015; Palenciano et al., 2019a). Importantly, the
612 competition level could be differentiated in most of the preparation window. However, it is
613 worth noting that these results could also be driven by other variables that may be
614 systematically modulated by competition levels. That is the case for instance of arousal, which
615 could be increased in high competition blocks. Also, our blocked design makes it highly likely
616 that the control settings (i.e., the overall task set of high vs. low competition contexts) were
617 maintained throughout the whole duration of the block (Dosenbach et al., 2008; Palenciano et
618 al., 2019b). Further studies will be needed to disentangle the differences between control
619 settings with various competition levels and arousal changes.

620 Unexpectedly, the temporal generalization profile of the overall competition context was
621 asymmetric, showing more generalization when the classifier was trained at the end of the
622 interval than for the reverse direction (Fig. 3B). This could be due to more stable preparatory
623 patterns at the end than at the beginning of the interval. However, earlier time points still

624 resulted in higher accuracy values, which may be caused by having a set of processes occurring
625 at the same time, which might be different for high and low competition contexts. Some of these
626 early cognitive processes might include physically perceiving the cue, remembering its
627 meaning, recalling the competition condition in which the participant is and preparing to
628 perceive the target and respond to it. As this set of processes might be taking place at the same
629 time only at the beginning of the interval, generalization to the rest of the time window may not
630 be possible. However, as the preparatory interval was fixed, participants could predict target
631 appearance, therefore at the end of the preparation interval neural activity could reflect to a
632 greater extent preparatory processes, such as category-specific patterns shown at the decoding
633 associated with the target category. These patterns, observed upon completion of the interval,
634 may also appear (alongside others) at different points within the preparation interval, thus
635 exhibiting greater generalizability.

636 Our results also indicate the presence of specific preparatory patterns linked to the anticipated
637 category of the target to select, both in high and low competition contexts. This is consistent
638 with the theory of biased competition, as a reflection of an internal attentional template
639 associated to the relevant category. Preparation is specific to the content of the incoming target
640 to select (González-García et al., 2017; Palenciano et al., 2019a; Peelen & Kastner, 2011;
641 Peñalver et al., 2023; Rajan et al., 2021; Sobrado et al., 2022; Stokes et al., 2009), with a
642 strength of category anticipation increasing at the end of the interval, in a ramping-up fashion,
643 replicating Peñalver and colleagues (2023). Although understanding the implications of this
644 finding requires further research, it could be related to temporal expectations. As mentioned
645 earlier, the preparatory interval was fixed, consequently the predictable temporal structure of the
646 task could intensify the preactivation of specific stimulus patterns towards target appearance
647 (Jin et al., 2020; Rohenkohl et al., 2012). Another possible, non-exclusive mechanism is the
648 processing of the cue meaning. This may occur silently (Stokes et al., 2009) at the beginning of
649 the preparation interval as evidenced in reduced decoding accuracy, and it may reactivate when
650 needed just before the target. The temporal generalization matrices of the categories on both
651 competition contexts also display a progressively increasing generalization toward the end of
652 the preparatory interval, suggesting that the activity patterns were not only stronger, but also
653 more stable over time at later stages (King & Dehaene, 2014).

654 The comparison of the preparatory category coding in high and low competition did not detect
655 differences between conditions in either the fidelity of these patterns or their temporal stability.
656 Hence, these results suggest that the categorical attentional templates were equivalent across
657 competition contexts. Although unexpected, this result resonates with previous evidence
658 showing that attentional templates also arise in low competition contexts (González-García et
659 al., 2016). Given that predictive cues were used in both contexts, it is reasonable that the
660 representation of target category was found in both situations. While the classifier accuracy
661 remained undistinguishable across contexts, the anticipated competition introduces other
662 differentiated process that might not be captured by the classifier alone, implying a multi-
663 faceted approach to information representation. Critically, finding equivalent classification
664 accuracies does not imply that the underlying neural codes are similar. This was supported by
665 the null results obtained with the cross-classification of category patterns between high and low
666 competition. The lack of significant clusters in the diagonal of the matrix, with only small
667 scattered clusters on the time generalization matrix, suggests that the anticipated category
668 coding in each of the contexts was not alike. Overall, this indicates that although the fidelity of
669 the anticipated content may be the same in high and low competition contexts, the underlying
670 patterns are not shared across conditions, implying a partially different format of preparation
671 depending on the context. Future studies are needed to further confirm this possible explanation.
672 On this respect, task demands could influence how the anticipated information is represented to
673 adapt to the context of the incoming target (Peñalver et al., 2023).

674 Analysis of the overlap between activity patterns from the perceptual localizer and preparation
675 interval of the main task allowed to examine whether the nature of the category-specific
676 anticipation was similar to perceptually driven patterns (Kaplan et al., 2015; Palenciano et al.,
677 2023). Results showed similarities between perceptual and preparatory category patterns in high
678 competition. Few small clusters were found in low competition. However, there was no
679 statistical evidence of differences between both conditions, which could be due to lack of power
680 to detect small differences in accuracy. Regarding high competition, the overlap between
681 preparatory and visual templates could be associated with the activation of perceptual regions
682 during preparation, as a perceptual reinstatement (Kerrén et al., 2018; Muckli et al., 2015; Smith
683 & Muckli, 2010; Vetter et al., 2014). The partial similarities between preparatory templates and
684 perceptual ones, in the anticipation of high stimuli competition, constitute a relevant finding that
685 contributes to a better understanding of the internal preparatory templates.

686 Turning to oscillatory activity, how anticipation of competition affects this activity had not been
687 explored in detail in the past. Theta power has been repeatedly related with effort or cognitive
688 control (Cavanagh & Frank, 2014; Cohen & Donner, 2013). Previous studies found that
689 preparing for a difficult task in which stimuli competition is high (Van Driel et al., 2015) or that
690 requires goal updating (Cooper et al., 2017) also induces an anticipatory increase in theta power.
691 Relatedly, and in accordance with our hypothesis, we found that preparing for high competition
692 generated increased theta power in all the preparation interval. Interestingly, this large cluster
693 started right at the beginning of the cue presentation. While this could reflect some extent of
694 smearing of the signal induced by the time-frequency decomposition, this would be unlikely
695 given the high temporal precision for estimating low frequencies such as theta, as the number of
696 cycles assigned to these bands is quite low. Instead, it could be driven by the blocked design
697 employed, which facilitated maintaining the different competition control settings over several
698 trials (Dosenbach et al., 2008; Palenciano et al., 2019b). This temporal profile contrasts with the
699 category-specific anticipation patterns, that are decodable only at the end of the window.
700 Importantly, our results show that these two different preparatory mechanisms are not
701 correlated. This finding, together with the previously described results, suggest that they reflect
702 different proactive processes that contribute distinctively based on the task requirements. Theta
703 power could implement more general control signals, associated with the general level of
704 competition, whereas category preactivations are specific to the content anticipated (Weber et
705 al., 2024).

706 Regarding the relationship between anticipatory neural patterns and behavioral performance,
707 some studies suggest that the better these indices, the better task performance (González-García
708 et al., 2017; Manelis & Reder, 2015; Peelen & Kastner, 2011; Soon et al., 2013; Stokes et al.,
709 2009). Our results, however, show inconclusive evidence on this respect. Neither preparatory
710 patterns coding the competition level nor the selected category correlated with behavioral
711 measurements. This was also the case for the correlations with the behavioral congruency effect.
712 This may suggest that the fidelity with which the brain preactivates specific categorical
713 templates of the target does not have a direct influence on the efficiency of behavior, which is in
714 contrast with other studies (González-García et al., 2017; Manelis & Reder, 2015; Peelen &
715 Kastner, 2011). However, the current paradigm was not tailored to entail a wide range of
716 decoding variability in the results, which could hinder the detection of associations between
717 subtle neural preactivations and behavioral measures. Further research is necessary to further
718 explore these associations.

719 Results show that the neural mechanisms reflected by theta power, in contrast, play an
720 important role for behavioral performance. The effect of competition on RT is partially caused
721 by power in the theta band, indicating that high competition is related to higher theta power
722 which in turn partially explains responses. This finding is in line with previous studies on
723 cognitive control (Cohen & Donner, 2013; Formica et al., 2022). A significant distinction in

724 analyzing the relationship between theta and behavior, compared to the decoding-behavior
725 relation, lies in the utilization of trial-by-trial data in the theta analysis. Obtaining a single value
726 per trial, especially when employing cross-classification to study category-specific patterns, is
727 challenging in the decoding analysis. Other studies have extracted d-values to be more precise
728 (Kerrén et al., 2018; Linde-Domingo et al., 2019; Ritchie et al., 2015), however as we
729 performed cross-classification across cue shapes, this was not feasible. Further tailored studies
730 could address optimal procedures for extracting trial-wise a d-values for the anticipatory neural
731 patterns without visual confounds.

732 The present study has limitations that restrict the reach of the findings and may catalyze further
733 investigations. First, our scope was the temporal domain, therefore we focused our analyses on
734 the temporal profile of preparatory activity. Further studies may complement our findings with
735 spatially resolved techniques, increasing the anatomical specificity of the different preparatory
736 mechanisms according to competition levels. Moreover, additional studies could use more
737 diverse stimuli over faces and names, and investigate the role of differential difficulty across
738 stimulus categories, which may interact with the competition effect (e.g. Zhang et al., 2013).
739 Although the current study is not optimized to address this issue, our AUC metric avoids any
740 bias towards a particular stimulus type. Related to this, it may be of interest including
741 multisensory stimuli such as visual and auditory combinations, to replicate and extend the
742 findings to other sensory domains. Furthermore, naturalistic contexts that include different
743 levels of competition could be key to transfer the results to the real environment (Graumann et
744 al., 2022, 2023). Lastly, although our study focuses on preparatory activity, it would be
745 interesting to explore the relationship between attentional templates and target processing. This
746 was not possible on the current dataset because the target-distractor display was substantially
747 different across competition conditions. Future studies could address this issue by reducing the
748 visual differences between conditions. This kind of experiment would enable the examination of
749 the roles played by preparatory attentional templates and anticipatory theta power during actual
750 target processing.

751 **4.1. Conclusion**

752 Overall, our results provide insights into how preparation differs depending on the difficulty of
753 the competition that is anticipated. The levels of competition exert a proactive influence on
754 multivariate neural patterns and theta activity. Moreover, the neural mechanisms underlying
755 theta oscillatory activity impact the efficiency of behavior. Integrating these findings into
756 theoretical models of selective attention is crucial for a comprehensive understanding of top-
757 down processes across contexts.

758

759 **Author statement**

760 **Blanca Aguado-López:** Data curation, Formal analysis, Writing -original draft. **Ana F. Palenciano:** Formal analysis, Writing -review & editing, Supervision. **José M.G. Peñalver:** Conceptualization, Methodology, Software programming, Data curation, Formal analysis. **Paloma Díaz-Gutiérrez:** Conceptualization, Methodology, Software programming. **David López-García:** Formal analysis. **Chiara Avancini:** Formal analysis. **Luis F. Ciria:** Formal analysis. **María Ruz:** Conceptualization, Methodology, Resources, Writing -review & editing, Supervision, Project administration, Funding acquisition.

767 **Open practices section**

768 The original data, task, and analysis scripts are openly available. Original code for the EEG
769 preprocessing has been posted on our team Github (<https://github.com/Human-Neuroscience/eeg-preprocessing>). Raw EEG data, organized following the BIDS format (Pernet
770

771 et al., 2019) will be deposited in the OpenNeuro public server once the paper is published. The
772 analysis code, results and task code are shared in an Open Science Framework repository that
773 will be public once the paper is published.

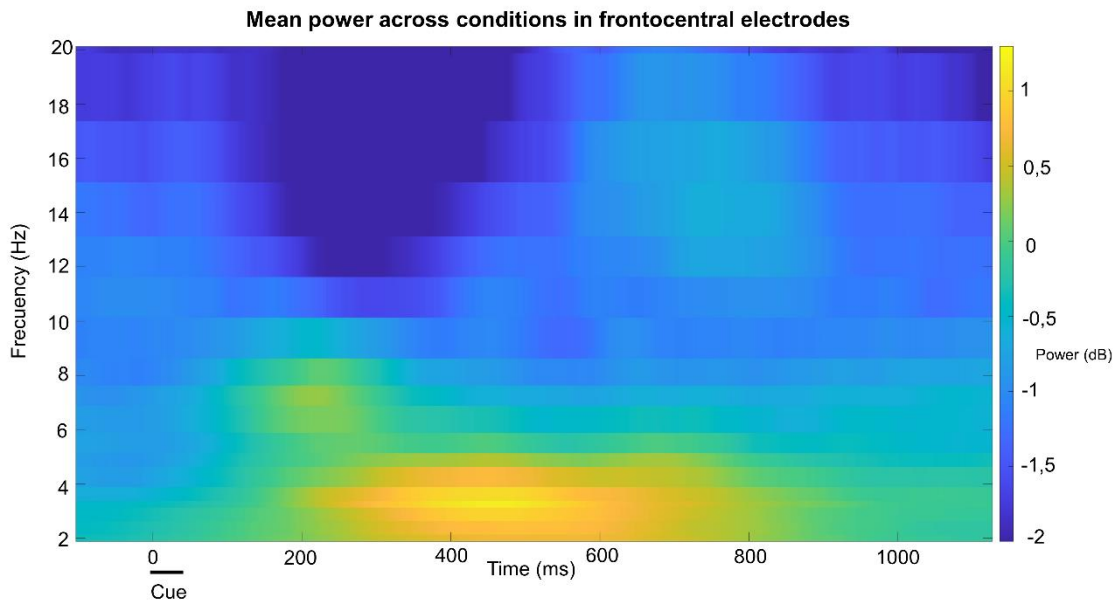
774 **Declaration of competing interest**

775 The authors declare no competing interests.

776 **Acknowledgements and fundings**

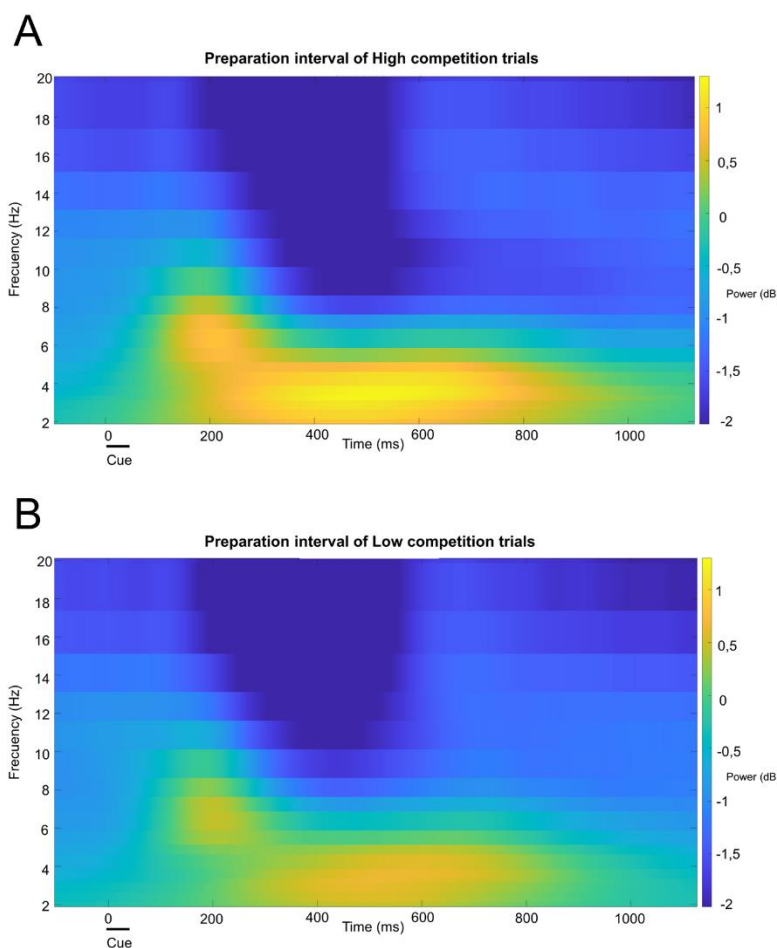
777 This research was supported by grants PID2019-111187GB-100, PID2022-138940NB, funded
778 by MICIU/AEI/ 10.13039/501100011033 and FEDER, UE, awarded to MR. BAL is supported
779 by a scholarship from the Spanish Ministry of Universities (FPU20/01980). AFP was supported
780 by Grant PAIDI21_00207 of the Andalusian Autonomic Government. JMGp was supported by
781 a scholarship from the Spanish Ministry of Universities (FPU18/01853). CA was supported by a
782 postdoctoral fellowship by the Spanish Ministry for Science and Innovation (FJC2020-046310-
783 I). We are grateful to Christopher I. Williamson for his assistance in data collection.

784 **Supplementary material**



785

786 **Fig. S1.** Results of the time-frequency analysis averaged across conditions and participants
787 during the cue-locked window, from -100 ms to 1125 ms.



788

789 **Fig. S2.** Results of the time-frequency analysis in the preparation epoch of High (A) and Low
790 competition trials from -100 ms to 1125 ms, averaged across participants.

791

792

793 **Supplementary results: LMM equations and results**

794 In our first model we tested if, controlling for congruency, there was an effect of task on RTs,
795 putting a random slope for competition and a random intercept for each participant ($RT \sim$
796 competition + congruency + (competition | subject)). In agreement with previous analysis, Low
797 competition blocks were responded faster than High competition ones ($t_{35.12} = 4.769$, $\beta = 0.021$,
798 CI 95% = [0.012, 0.030], $p < 0.001$). Congruency was also significant ($t_{30807} = -15.189$, $\beta = -$
799 0.018, CI 95% = [-0.020, -0.015], $p < 0.001$). Second, we tested if there was an effect of
800 competition on theta, by fitting an LMM with the same structure but predicting the trial-wise
801 theta values (theta \sim competition + congruency + (competition | subject)). The effect of
802 competition on theta was also significant, so that High competition induced higher theta power
803 ($t_{34.7} = 3.793$, $\beta = 0.19$, CI 95% = [0.092, 0.289], $p < 0.001$). Third, we tested the fixed effects of
804 theta and competition on RTs, also controlling congruency with the same random structure (RT
805 \sim theta + competition + congruency + (competition | subject)). The effect of theta was
806 significant ($t_{30824.2} = -2.86$, $\beta = -0.001$, CI 95% = [-0.001, -0.0002], $p < 0.01$), suggesting that
807 larger theta values were associated with faster responses. There was also a main effect of
808 competition ($t_{35.1} = 4.807$, $\beta = 0.021$, CI 95% = [0.013, 0.030], $p < 0.001$) and an effect of
809 congruency ($t_{30806} = -15.187$, $\beta = -0.018$, CI 95% = [-0.02, -0.015], $p < 0.001$).

810

811 **References**

812 Baron, R. M., & Kenny, D. A. (1986). The moderator–mediator variable distinction in social
813 psychological research: Conceptual, strategic, and statistical considerations. *Journal of
814 personality and social psychology*, 51(6), 1173.

815 Barr, D. J., Levy, R., Scheepers, C., & Tily, H. J. (2013). Random effects structure for
816 confirmatory hypothesis testing: Keep it maximal. *Journal of Memory and Language*,
817 68(3), 255–278. <https://doi.org/10.1016/j.jml.2012.11.001>

818 Bates D, Mächler M, Bolker BM, Walker SC (2014) Fitting linear mixed-effects models using
819 lme4. *J Stat Softw* 67:1–48.

820 Beck, D. M., & Kastner, S. (2009). Top-down and bottom-up mechanisms in biasing
821 competition in the human brain. *Vision Research*, 49(10), 1154–1165.
822 <https://doi.org/10.1016/j.visres.2008.07.012>

823 Brainard, D. H. (1997). The Psychophysics Toolbox. *Spatial Vision*, 10(4), 433–436.
824 <https://doi.org/10.1163/156856897X00357>

825 Braver, T. S. (2012). The variable nature of cognitive control: A dual mechanisms framework.
826 *Trends in Cognitive Sciences*, 16(2), 106–113.
827 <https://doi.org/10.1016/j.tics.2011.12.010>

828 Cavanagh, J. F., & Frank, M. J. (2014). Frontal theta as a mechanism for cognitive control.
829 *Trends in Cognitive Sciences*, 18(8), 414–421.
830 <https://doi.org/10.1016/j.tics.2014.04.012>

831 Chevalier, N., Hadley, L. V., & Balthrop, K. (2021). Midfrontal theta oscillations and conflict
832 monitoring in children and adults. *Developmental Psychobiology*, 63(8), e22216.
833 <https://doi.org/10.1002/dev.22216>

834 Cohen, M. X. (2019). A better way to define and describe Morlet wavelets for time-frequency
835 analysis. *NeuroImage*, 199, 81–86. <https://doi.org/10.1016/j.neuroimage.2019.05.048>

836 Cohen, M. X., & Donner, T. H. (2013). Midfrontal conflict-related theta-band power reflects
837 neural oscillations that predict behavior. *Journal of Neurophysiology*, 110(12), 2752–
838 2763. <https://doi.org/10.1152/jn.00479.2013>

839 Cohen, M. X., & Van Gaal, S. (2014). Subthreshold muscle twitches dissociate oscillatory
840 neural signatures of conflicts from errors. *NeuroImage*, 86, 503–513.
841 <https://doi.org/10.1016/j.neuroimage.2013.10.033>

842 Cooper, P. S., Wong, A. S. W., McKewen, M., Michie, P. T., & Karayanidis, F. (2017).
843 Frontoparietal theta oscillations during proactive control are associated with goal-
844 updating and reduced behavioral variability. *Biological Psychology*, 129, 253–264.
845 <https://doi.org/10.1016/j.biopsych.2017.09.008>

846 Delorme, A., & Makeig, S. (2004). EEGLAB: An open source toolbox for analysis of single-
847 trial EEG dynamics including independent component analysis. *Journal of
848 Neuroscience Methods*, 134(1), 9–21. <https://doi.org/10.1016/j.jneumeth.2003.10.009>

849 Desimone, R., & Duncan, J. (1995). Neural Mechanisms of Selective Visual Attention. *Annual
850 review of neuroscience*, 18(1), 193–222.

851 Dosenbach, N. U., Fair, D. A., Cohen, A. L., Schlaggar, B. L., & Petersen, S. E. (2008). A dual-
852 networks architecture of top-down control. *Trends in cognitive sciences*, 12(3), 99–105.
853 <https://doi.org/10.1016/j.tics.2008.01.001>

854 Duncan, J. (1993). Similarity between concurrent visual discriminations: Dimensions and
855 objects. *Perception & Psychophysics*, 54(4), 425–430.
856 <https://doi.org/10.3758/BF03211764>

857 Eriksen, B. A., & Eriksen, C. W. (1974). Effects of noise letters upon the identification of a
858 target letter in a nonsearch task. *Perception & Psychophysics*, 16(1), 143–149.
859 <https://doi.org/10.3758/BF03203267>

860 Formica, S., González-García, C., Senoussi, M., Marinazzo, D., & Brass, M. (2022). Theta-
861 Phase Connectivity between Medial Prefrontal and Posterior Areas Underlies Novel

862 Instructions Implementation. *Eneuro*, 9(4), ENEURO.0225-22.2022.
863 <https://doi.org/10.1523/ENEURO.0225-22.2022>

864 González-García, C., Arco, J. E., Palenciano, A. F., Ramírez, J., & Ruz, M. (2017). Encoding,
865 preparation and implementation of novel complex verbal instructions. *NeuroImage*,
866 148, 264–273. <https://doi.org/10.1016/j.neuroimage.2017.01.037>

867 González-García, C., Mas-Herrero, E., De Diego-Balaguer, R., & Ruz, M. (2016). Task-specific
868 preparatory neural activations in low-interference contexts. *Brain Structure and*
869 *Function*, 221(8), 3997–4006. <https://doi.org/10.1007/s00429-015-1141-5>

870 Graumann, M., Ciuffi, C., Dwivedi, K., Roig, G., & Cichy, R. M. (2022). The spatiotemporal
871 neural dynamics of object location representations in the human brain. *Nature Human*
872 *Behaviour*, 6(6), 796–811. <https://doi.org/10.1038/s41562-022-01302-0>

873 Graumann, M., Wallenwein, L. A., & Cichy, R. M. (2023). Independent spatiotemporal effects
874 of spatial attention and background clutter on human object location representations.
875 *NeuroImage*, 272, 120053. <https://doi.org/10.1016/j.neuroimage.2023.120053>

876 Grootswagers, T., Wardle, S. G., & Carlson, T. A. (2017). Decoding Dynamic Brain Patterns
877 from Evoked Responses: A Tutorial on Multivariate Pattern Analysis Applied to Time
878 Series Neuroimaging Data. *Journal of Cognitive Neuroscience*, 29(4), 677–697.
879 https://doi.org/10.1162/jocn_a_01068

880 Groppe, D. M., Urbach, T. P., & Kutas, M. (2011). Mass univariate analysis of event-related
881 brain potentials/fields I: A critical tutorial review. *Psychophysiology*, 48(12), 1711–
882 1725. <https://doi.org/10.1111/j.1469-8986.2011.01273.x>

883 Hall-McMaster, S., Muhle-Karbe, P. S., Myers, N. E., & Stokes, M. G. (2019). Reward Boosts
884 Neural Coding of Task Rules to Optimize Cognitive Flexibility. *The Journal of*
885 *Neuroscience*, 39(43), 8549–8561. <https://doi.org/10.1523/JNEUROSCI.0631-19.2019>

886 Jackson, J., Rich, A. N., Williams, M. A., & Woolgar, A. (2017). Feature-selective Attention in
887 Frontoparietal Cortex: Multivoxel Codes Adjust to Prioritize Task-relevant Information.
888 *Journal of Cognitive Neuroscience*, 29(2), 310–321.
889 https://doi.org/10.1162/jocn_a_01039

890 Jin, W., Nobre, A. C., & Van Ede, F. (2020). Temporal Expectations Prepare Visual Working
891 Memory for Behavior. *Journal of Cognitive Neuroscience*, 32(12), 2320–2332.
892 https://doi.org/10.1162/jocn_a_01626

893 Kaiser, D., Oosterhof, N. N., & Peelen, M. V. (2016). The Neural Dynamics of Attentional
894 Selection in Natural Scenes. *The Journal of Neuroscience*, 36(41), 10522–10528.
895 <https://doi.org/10.1523/JNEUROSCI.1385-16.2016>

896 Kaplan, J. T., Man, K., & Greening, S. G. (2015). Multivariate cross-classification: Applying
897 machine learning techniques to characterize abstraction in neural representations.
898 *Frontiers in Human Neuroscience*, 9. <https://doi.org/10.3389/fnhum.2015.00151>

899 Kastner, S., De Weerd, P., Desimone, R., & Ungerleider, L. G. (1998). Mechanisms of Directed
900 Attention in the Human Extrastriate Cortex as Revealed by Functional MRI. *Science*,
901 282(5386), 108–111. <https://doi.org/10.1126/science.282.5386.108>

902 Kerrén, C., Linde-Domingo, J., Hanslmayr, S., & Wimber, M. (2018). An Optimal Oscillatory
903 Phase for Pattern Reactivation during Memory Retrieval. *Current Biology*, 28(21),
904 3383–3392.e6. <https://doi.org/10.1016/j.cub.2018.08.065>

905 King, J. R., Faugeras, F., Gramfort, A., Schurter, A., El Karoui, I., Sitt, J. D., Rohaut, B.,
906 Wacongne, C., Labyt, E., Bekinschtein, T., Cohen, L., Naccache, L., & Dehaene, S.
907 (2013). Single-trial decoding of auditory novelty responses facilitates the detection of
908 residual consciousness. *NeuroImage*, 83, 726–738.
909 <https://doi.org/10.1016/j.neuroimage.2013.07.013>

910 King, J. R., & Dehaene, S. (2014). Characterizing the dynamics of mental representations: The
911 temporal generalization method. *Trends in Cognitive Sciences*, 18(4), 203–210.
912 <https://doi.org/10.1016/j.tics.2014.01.002>

913 Li, Q., Wang, J., Li, Z., & Chen, A. (2022). Decoding the Specificity of Post-Error Adjustments
914 Using EEG-Based Multivariate Pattern Analysis. *The Journal of Neuroscience*, 42(35),
915 6800–6809. <https://doi.org/10.1523/JNEUROSCI.0590-22.2022>

916 Linde-Domingo, J., Treder, M. S., Kerrén, C., & Wimber, M. (2019). Evidence that neural
917 information flow is reversed between object perception and object reconstruction from
918 memory. *Nature Communications*, 10(1), 179. <https://doi.org/10.1038/s41467-018-08080-2>

920 López-García, D., Peñalver, J. M. G., Górriz, J. M., & Ruz, M. (2022). MVPAlab: A machine
921 learning decoding toolbox for multidimensional electroencephalography data. *Computer
922 Methods and Programs in Biomedicine*, 214, 106549.
923 <https://doi.org/10.1016/j.cmpb.2021.106549>

924 López-García, D., Sobrado, A., Peñalver, J. M. G., Górriz, J. M., & Ruz, M. (2020).
925 Multivariate Pattern Analysis Techniques for Electroencephalography Data to Study
926 Flanker Interference Effects. *International Journal of Neural Systems*, 30(07), 2050024.
927 <https://doi.org/10.1142/S0129065720500240>

928 Love, J., Selker, R., Marsman, M., Jamil, T., Dropmann, D., Verhagen, J., Ly, A., Gronau, Q.
929 F., Smíra, M., Epskamp, S., Matzke, D., Wild, A., Knight, P., Rouder, J. N., Morey, R.
930 D., & Wagenmakers, E.-J. (2019). JASP: Graphical Statistical Software for Common
931 Statistical Designs. *Journal of Statistical Software*, 88(2).
932 <https://doi.org/10.18637/jss.v088.i02>

933 Luke, S. G. (2017). Evaluating significance in linear mixed-effects models in R. *Behavior
934 Research Methods*, 49(4), 1494–1502. <https://doi.org/10.3758/s13428-016-0809-y>

935 Ma, D. S., Correll, J., & Wittenbrink, B. (2015). The Chicago face database: A free stimulus set
936 of faces and norming data. *Behavior Research Methods*, 47(4), 1122–1135.
937 <https://doi.org/10.3758/s13428-014-0532-5>

938 Manelis, A., & Reder, L. M. (2015). He Who Is Well Prepared Has Half Won The Battle: An
939 fMRI Study of Task Preparation. *Cerebral Cortex*, 25(3), 726–735.
940 <https://doi.org/10.1093/cercor/bht262>

941 Maris, E., & Oostenveld, R. (2007). Nonparametric statistical testing of EEG- and MEG-data.
942 *Journal of Neuroscience Methods*, 164(1), 177–190.
943 <https://doi.org/10.1016/j.jneumeth.2007.03.024>

944 Moore, M. J., Robinson, A. K., & Mattingley, J. B. (2024). Expectation modifies the
945 representational fidelity of complex visual objects. *Imaging Neuroscience*.
946 https://doi.org/10.1162/imag_a_00083

947 Moran, J., & Desimone, R. (1985). Selective attention gates visual processing in the extrastriate
948 cortex. *Science*, 229(4715), 782–784.

949 Muckli, L., De Martino, F., Vizioli, L., Petro, L. S., Smith, F. W., Ugurbil, K., Goebel, R., &
950 Yacoub, E. (2015). Contextual Feedback to Superficial Layers of V1. *Current Biology*,
951 25(20), 2690–2695. <https://doi.org/10.1016/j.cub.2015.08.057>

952 Nigbur, R., Cohen, M. X., Ridderinkhof, K. R., & Stürmer, B. (2012). Theta Dynamics Reveal
953 Domain-specific Control over Stimulus and Response Conflict. *Journal of Cognitive
954 Neuroscience*, 24(5), 1264–1274. https://doi.org/10.1162/jocn_a_00128

955 Nigbur, R., Ivanova, G., & Stürmer, B. (2011). Theta power as a marker for cognitive
956 interference. *Clinical Neurophysiology*, 122(11), 2185–2194.
957 <https://doi.org/10.1016/j.clinph.2011.03.030>

958 Palenciano, A. F., González-García, C., Arco, J. E., Pessoa, L., & Ruz, M. (2019a).
959 Representational Organization of Novel Task Sets during Proactive Encoding. *The
960 Journal of Neuroscience*, 39(42), 8386–8397.
961 <https://doi.org/10.1523/JNEUROSCI.0725-19.2019>

962 Palenciano, A. F., González-García, C., Arco, J. E., & Ruz, M. (2019b). Transient and sustained
963 control mechanisms supporting novel instructed behavior. *Cerebral Cortex*, 29(9),
964 3948–3960. <https://doi.org/10.1093/cercor/bhy273>

965 Palenciano, A. F., Senoussi, M., Formica, S., & González-García, C. (2023). Canonical template
966 tracking: Measuring the activation state of specific neural representations. *Frontiers in*
967 *Neuroimaging*, 1, 974927. <https://doi.org/10.3389/fnimg.2022.974927>

968 Peelen, M. V., & Kastner, S. (2011). A neural basis for real-world visual search in human
969 occipitotemporal cortex. *Proceedings of the National Academy of Sciences*, 108(29),
970 12125–12130. <https://doi.org/10.1073/pnas.1101042108>

971 Peñalver, J. M. G., López-García, D., González-García, C., Aguado-López, B., Górriz, J. M., &
972 Ruz, M. (2023). Top-down specific preparatory activations for selective attention and
973 perceptual expectations. *NeuroImage*, 271, 119960.
974 <https://doi.org/10.1016/j.neuroimage.2023.119960>

975 Peñalver, J. M. G. (2024). *Neural Mechanisms of Preparation in Expectation and Selective*
976 *Attention* [Unpublished doctoral thesis]. Universidad de Granada.

977 Pernet, C. R., Appelhoff, S., Gorgolewski, K. J., Flandin, G., Phillips, C., Delorme, A., &
978 Oostenveld, R. (2019). EEG-BIDS, an extension to the brain imaging data structure for
979 electroencephalography. *Scientific data*, 6(1), 103. <https://doi.org/10.1038/s41597-019-0104-8>

981 Rajan, A., Meyyappan, S., Liu, Y., Samuel, I. B. H., Nandi, B., Mangun, G. R., & Ding, M.
982 (2021). The Microstructure of Attentional Control in the Dorsal Attention Network.
983 *Journal of Cognitive Neuroscience*, 33(6), 965–983.
984 https://doi.org/10.1162/jocn_a_01710

985 Reddy, L., Kanwisher, N. G., & VanRullen, R. (2009). Attention and biased competition in
986 multi-voxel object representations. *Proceedings of the National Academy of Sciences*,
987 106(50), 21447–21452. <https://doi.org/10.1073/pnas.0907330106>

988 Ritchie, J. B., Tovar, D. A., & Carlson, T. A. (2015). Emerging Object Representations in the
989 Visual System Predict Reaction Times for Categorization. *PLOS Computational*
990 *Biology*, 11(6), e1004316. <https://doi.org/10.1371/journal.pcbi.1004316>

991 Richmond, B. J., Wurtz, R. H., & Sato, T. (1983). Visual responses of inferior temporal neurons
992 in awake rhesus monkey. *Journal of neurophysiology*, 50(6), 1415–1432.

993 Rohenkohl, G., Cravo, A. M., Wyart, V., & Nobre, A. C. (2012). Temporal Expectation
994 Improves the Quality of Sensory Information. *Journal of Neuroscience*, 32(24), 8424–
995 8428. <https://doi.org/10.1523/JNEUROSCI.0804-12.2012>

996 Ruz, M., & Nobre, A. C. (2008). Dissociable top-down anticipatory neural states for different
997 linguistic dimensions. *Neuropsychologia*, 46(4), 1151–1160.
998 <https://doi.org/10.1016/j.neuropsychologia.2007.10.021>

999 Sheldon, A. D., Saad, E., Sahan, M. I., Meyering, E. E., Starrett, M. J., LaRocque, J. J., Rose, N.
1000 S., & Postle, B. R. (2021). Attention Biases Competition for Visual Representation via
1001 Dissociable Influences from Frontal and Parietal Cortex. *Journal of Cognitive*
1002 *Neuroscience*, 33(4), 739–755. https://doi.org/10.1162/jocn_a_01672

1003 Simon, J.R. (1969). Reactions toward the source of stimulation. *Journal of Experimental*
1004 *Psychology*, 81(1), 174–6

1005 Smith, F. W., & Muckli, L. (2010). Nonstimulated early visual areas carry information about
1006 surrounding context. *Proceedings of the National Academy of Sciences*, 107(46),
1007 20099–20103. <https://doi.org/10.1073/pnas.1000233107>

1008 Sobrado, A., Palenciano, A. F., González-García, C., & Ruz, M. (2022). The effect of task
1009 demands on the neural patterns generated by novel instruction encoding. *Cortex*, 149,
1010 59–72. <https://doi.org/10.1016/j.cortex.2022.01.010>

1011 Soon, C. S., Namburi, P., & Chee, M. W. L. (2013). Preparatory patterns of neural activity
1012 predict visual category search speed. *NeuroImage*, 66, 215–222.
1013 <https://doi.org/10.1016/j.neuroimage.2012.10.036>

1014 Stokes, M., Thompson, R., Nobre, A. C., & Duncan, J. (2009). Shape-specific preparatory
1015 activity mediates attention to targets in human visual cortex. *Proceedings of the*
1016 *National Academy of Sciences*, 106(46), 19569–19574.
1017 <https://doi.org/10.1073/pnas.0905306106>

1018 Tingley, D., Yamamoto, T., Hirose, K., Keele, L., & Imai, K. (2014). Mediation: R package for
1019 causal mediation analysis.

1020 Van Driel, J., Swart, J. C., Egner, T., Ridderinkhof, K. R., & Cohen, M. X. (2015). (No) time
1021 for control: Frontal theta dynamics reveal the cost of temporally guided conflict
1022 anticipation. *Cognitive, Affective, & Behavioral Neuroscience*, 15(4), 787–807.
1023 <https://doi.org/10.3758/s13415-015-0367-2>

1024 Vetter, P., Smith, F. W., & Muckli, L. (2014). Decoding Sound and Imagery Content in Early
1025 Visual Cortex. *Current Biology*, 24(11), 1256–1262.
1026 <https://doi.org/10.1016/j.cub.2014.04.020>

1027 Weber, J., Solbakk, A. K., Blenkmann, A. O., Llorens, A., Funderud, I., Leske, S., Larsson, P.
1028 G., Ivanovic, J., Knight, R. T., Endestad, T., & Helfrich, R. F. (2024). Ramping
1029 dynamics and theta oscillations reflect dissociable signatures during rule-guided human
1030 behavior. *Nature Communications*, 15(1), 637. <https://doi.org/10.1038/s41467-023-44571-7>

1032 Westfall, J. (2016). PANGEA: power ANalysis for GEneral Anova designs.

1033 Zhang, L., Ding, C., Li, H., Zhang, Q., & Chen, A. (2013). The influence of attentional control
1034 on stimulus processing is category specific in Stroop tasks: Attentional
1035 control. *Psychological research*, 77, 599–610. <https://doi.org/10.1007/s00426-012-0457-5>

1036